Chaotic antennas

Vadym Slyusar
Central Research Institute of Armaments and Military Equipment of Armed Forces of Ukraine
Kyiv, Ukraine
swadim@ukr.net

Ihor Sliusar
Department of information systems and technologies
Poltava State Agrarian Academy
Poltava, Ukraine
islyusar2007@ukr.net

Oleksii Nalapko
Central Research Institute of Armaments and Military Equipment of Armed Forces of Ukraine
Kyiv, Ukraine
aln.uax@gmail.com

***Abstract* — The paper proposes a new type of multiband broadband printed antennas with a chaotic outline. To synthesize them, the topologies for solving the traveling salesman problem based on the ant colony optimization algorithm are used. Removal of topological restrictions on the trajectory of traversing the matrix of cities made it possible to switch from meander-type antenna structures to antennas with chaotic geometry. In this case, the requirement on the restriction is fulfilled, according to which the trajectories of traversing the matrix of cities should not have mutual intersections. In the course of the research, several design options were considered, which differ in the variation of the antenna parameters. For their synthesis and analysis, the Numerical modeling methods were used due to the complexity of describing the interaction of antennas of non-Euclidean geometry with radio waves. Evaluation and comparison of proposed antennas held by the following characteristics: amplitude-frequency response and voltage standing wave ratio.**

Keywords— ant colony optimisation (ACO), travelling salesman problem, chaotic contour, chaotic patch antenna, Ansoft HFSS, amplitude-frequency response, voltage standing wave ratio, beam pattern.

I. INTRODUCTION

The development process of the 6th generation of mobile communication systems (6G) is closely related to the selection of new frequency bands for their operations. General 6G communication concepts typically operate at frequencies of 100 GHz and above [1 - 4]. However, it is quite obvious that before making such a leap in the spectrum, it is advisable, within the framework of subsequent releases of 5G standards, to gradually migrate communication equipment to the millimeter wavelength range with frequencies above 30 GHz. Among the publications specifying the possible values of such transient frequencies, it should be noted [3, 4]. For example, the authors of [4] pointed out the possibility of using frequencies within the framework of the transition from 5G to 6G not only in the 60 GHz region, which are already being mastered within the framework of IEEE 802.11ad, IEEE 802.15.3c, ECMA-387 and 5G NR standards, but also in the ranges 71 - 86 and 92 - 114.25 GHz.

It is quite obvious that the equipment of promising base stations and user devices for cellular communication will have to support the operation of several generations of systems simultaneously, in particular, various versions of 5G and 6G in combination with other data transmission standards. In this context, an urgent task is to develop the design of broadband antennas, which will technically implement multi-band reception and emission of signals in the indicated transition frequency zones, as to maintain the communication in traditional frequency ranges below 6 GHz as well.

II. ANALYSIS OF RECENT STUDIES AND PUBLICATIONS, WHICH DISCUSS THE PROBLEM

This report proposes a new type of printed antennas, called chaotic due to the peculiar geometry of their contour line, as possible applicants for antennas that meet the above requirements.

In terms of their frequency properties, the designs of chaotic printed antennas considered below occupy an intermediate niche between classical printed antennas with rectangular or round shapes and their modifications on the one hand [5, 6], as well as quasi-fractal designs of printed emitters [7] - on the other hand.

The synthesis of the topology of chaotic antennas was carried out on the basis of the application of the ant colony optimization (ACO) algorithm for solving the traveling salesman problem. It should be noted that the use of the capabilities of the ACO algorithm for antenna synthesis is not new in itself. For example, in [8, 9], this approach was used to synthesize loop antennas and open dipoles. However, in these publications, strict restrictions were imposed on the topology of the matrix of cities, which was a fixed square matrix of 10x10 format [8, 9]. At the same time, as a result of the functioning of the ACO algorithm, when solving the transport problem, only meander type antennas were obtained.

Meanwhile, in a more general form, the topology of the matrix of cities can be arbitrary, similar to the cut-out matrices considered in [10]. As a result of removing topological restrictions, trajectories of traversing the matrix of cities are transformed to a chaotic form [11]. As applied to the synthesis of antenna topologies within the framework of this approach, one should still apply the constraint used earlier in [8, 9], according to which the

978-1-6654-0682-6/21/$31.00 ©2021 IEEE

trajectories of traversing the matrix of cities should not have mutual intersections.

III. The Aim of Research

Thus, the purpose of the work is to create conditions for expanding the functionality of mobile communication systems through the use of chaotic antennas based on ant optimization algorithms.

IV. The Main Results of the Study

As an example of the implementation of this synthesis concept, we will further consider a printed antenna with a chaotic outline shown in Fig. 1.

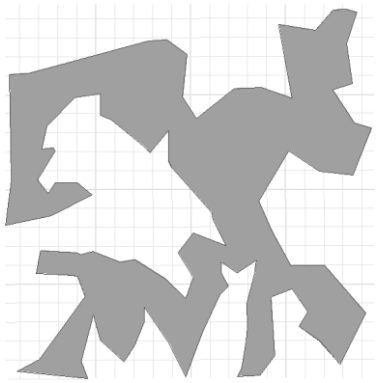

Fig. 1. The chaotic antenna contour.

The indicated contour was synthesized with the following parameters of the ACO algorithm:

– the number of vertices (cities) – 100;

– the number of iterations (generations of ants) – 2000;

– the number of ants in the one generation – 10;

– the odor alpha coefficient – 1 (by 0 the orientation is carried out only on the shortest path);

– the beta coefficient of distance is 2 (at 0, ants are guided only by smell);

– the coefficient of the global renewal of pheromone – 0.1;

– the coefficient of the local renewal of pheromone – 0.1;

– the number of pheromones left by one ant – 1.

In this case, every ant chooses a vertex (city) of the start randomly by placing at most one ant into one city.

In the course of the research, several options for the design of the printed antenna shown in Fig. 1 were considered. Among the varied parameters were used: the angle of a rotation of the antenna around its conditional center relative to the feeder; a feeder line connection point; the screen height; the geometric dimensions of the segments of the feeder line and the groove in the ground for its coordination; tilt angle and th height of the cuts at edges of the screen; dimensions and thickness of the substrate; its relative permittivity; ground thickness, scaling factor of antenna and feeder line dimensions.

To simulate the antennas, the Ansoft EMT 2020 environment was used, which is a further development of Ansys HFSS [12]. At the same time, the coordinates of the contour vertices obtained as a result of the functioning of the ACO algorithm were loaded through an intermediate Excel file into the CAD package to generate the corresponding image and then into the Ansoft EMT package.

To the comparison with the previously obtained results, a traditional printed antenna of square topology (Fig. 2) with a 50-ohm Lumped-type power port was considered as an object of comparison. At the same time, its dimensions were chosen in such a way that the contour of the chaotic antenna shown in Fig. 1, could be inscribed in the indicated square.

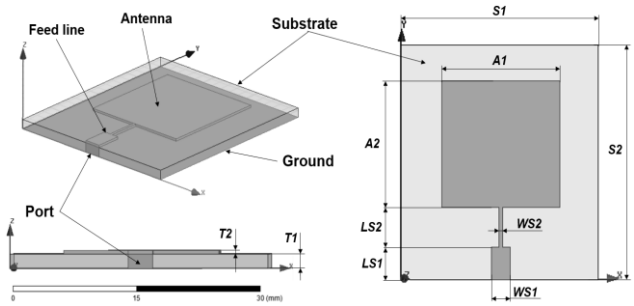

Fig. 2. Square printed antenna adopted as a reference for comparison.

According to [13, 14], to determine the efficiency of synthesized antenna solutions, it is advisable to carry out an analysis based on Return Loss (RL) and Voltage Standing Wave Ratio (VSWR). The fractional bandwidth parameter can be used to determine the antenna bandwidth level [15]:

$$\delta F = \frac{2|f_1 - f_2|}{f_1 + f_2},$$

where f_1 and f_2 – are the values of the frequencies at which the magnitude of the VSWR or RL exceeds a predetermined level.

Thus, the RL estimate for a square antenna (Fig. 2) is shown in Fig. 3.

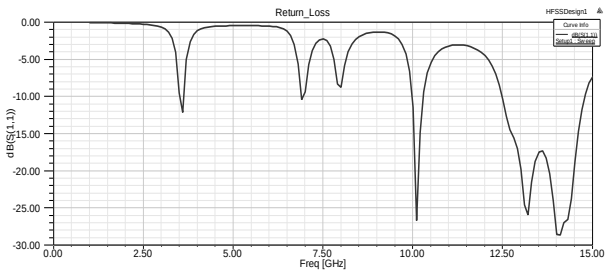

Fig. 3. Frequency dependence of RL of a square printed antenna.

As a starting point for further research, we chose the design of a chaotic antenna with a full sizes ground over the entire area of the substrate (Fig. 4), deployed to connect feeder 180 degrees with respect to Fig. 1.

The frequency dependence of its return loss is illustrated in Fig. 5. Geometrical parameters of the antenna are presented in the Table 1.

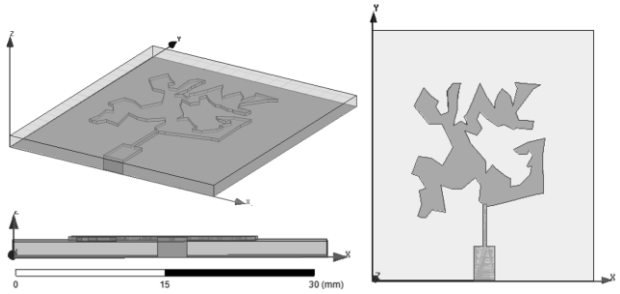

Fig. 4. The first iteration of a chaotic antenna with a full sizes ground.

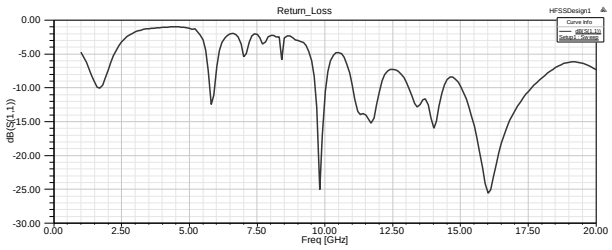

Fig. 5. The frequency dependence of RL for the antenna in Fig. 4.

TABLE I. ANTENNA PROPERTIES (FIG. 1 AND 4)

Element	Description
Substrate	FR4 (ε_r = 4.4), *T1* = 1.6 mm, *S1* = 36 mm, *S2* = 32 mm
Antenna	Cooper, *T2* = 0.389 mm, *A1* = 19.5 mm, *A2* = 19.5mm
Feed line	Cooper, *LS1* = 4.9 mm, *WS1* = 3 mm, *LS2* = 6.15 mm, *WS2* = 0.5 mm
Ground	Cooper, *G1* = *S1*, *G2* = *S2*

The comparison with a rectangular antenna shows that the significant advantages of the chaotic antenna in Fig. 4 is not observed in the considered frequency range. The difference lies in the presence of three sub-bands above the pronounced resonance around 10 GHz. In this regard, further research was aimed at optimizing the design and design parameters of the chaotic antenna. It should be noted that taking into account the existence of several interpretations of the bandwidth, its definition was used in the work on the basis of the return loss criterion, for which the S11 module is less than -10 dB (although more precisely the level of VSWR ≤ 2 corresponds to the value RL ≤ -9.542 dB). As a result, for the convenience of visualizing the results, VSWR estimates are mainly used in the work.

In the search for a suitable antenna design, the initial changes were in the area occupied by the ground. The shortened screen (Fig. 6) is described by the dimensions: G1 = S1 and G2 < S2.

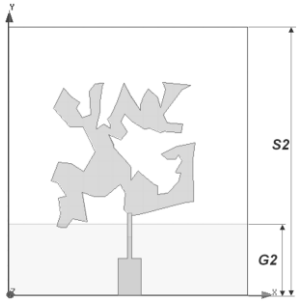

Fig. 6. The shortened ground of the chaotic antenna.

Of greatest interest were the variations with G2 ranging from LS1 to (LS1 + LS2). Decreasing the ground height to the "butt" position with the projection of the antenna contour (in the xOy plane) led to the appearance of a continuous antenna matching band in the 15 – 24 GHz range (Fig. 7).

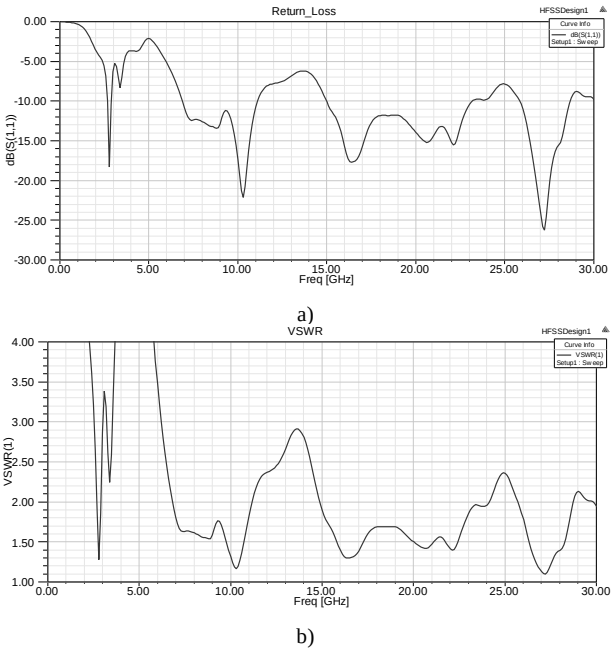

Fig. 7. Frequency dependences for an antenna with ground, which ends abut with the projection of the antenna (G2 = 9.077 mm): a) – RL, b) – VSWR.

The comparison with the square antenna shows that the chaotic contour in the case of its positioning end-to-end with the projection of the printed screen has a pronounced advantage in the frequency selectivity (Fig. 8).

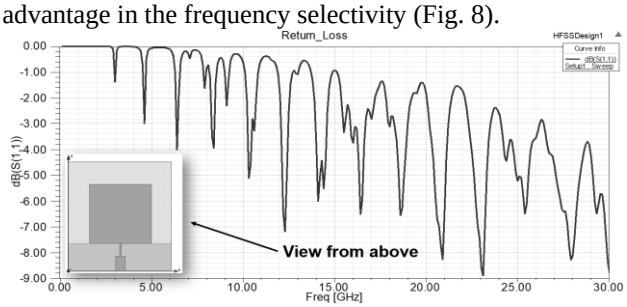

Fig. 8. Frequency dependence of RL of the square antenna, located end-to-end with ground. (*G2* = 9.07697 mm).

However, the best variant of the chaotic antenna design, taking into account the coverage of the zone of interest in the millimeter-wave range, was achieved with G2 = 9.3 mm (Fig. 9) and optimization of the connection point of the feeder line to the antenna body. The corresponding operating frequency band has expanded from 15 to 38 GHz.

At the next stage of research, manipulations with the height of the ground screen were supplemented by making a notch in its surface in the region of the projection of the upper segment of the supply line (Fig. 10).

This technique, similarly to [7], made it possible to improve its matching. As a result, for example, with a screen height of 9.2 mm, it was possible to eliminate the bounce in the frequency response in the region of 25 GHz

and to achieve the continuity of the bandwidth of the chaotic antenna in the section from 19 to 62 GHz (Fig. 11).

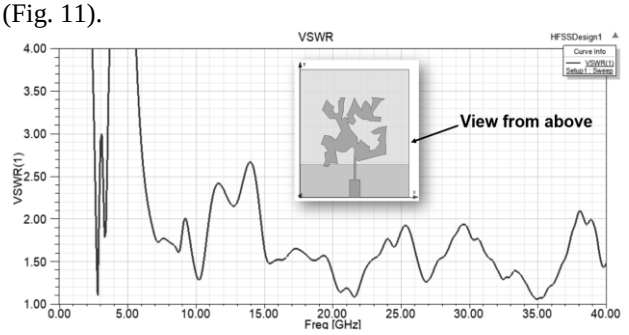

Fig. 9. VSWR frequency dependence of a chaotic antenna at *G2* = 9.3 mm.

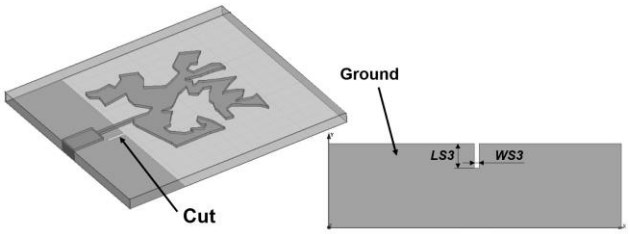

Fig. 10. The ground screen with a cutout.

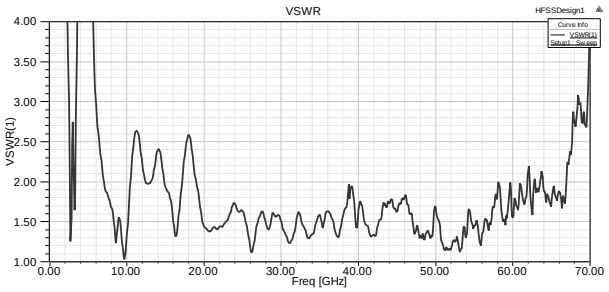

Fig. 11. The result of adding a cutout to the ground screen (*G2* = 9.2 mm, *LS3* = 2.7 mm, *WS3* = 0.54 mm).

After identifying mechanisms to achieve a wide millimeter-wave bandwidth, further efforts were focused on the finding of solutions to improve the spectral selectivity at frequencies below 10 GHz.

For this, the ground screen has been modified in the work by introducing symmetric angular cuts [7], as shown in Fig. 12. It is essential that in this case the printed antenna can be interpreted as a monopole located on the substrate in the form of a supply line with a capacitive load based on a chaotic outline. This approach made it possible to improve the frequency properties of the synthesized model of a chaotic antenna (Fig. 13): the lower limit of the passband decreased from 19 to 14.98 GHz, and the upper limit increased from 62 to 71.51 GHz.

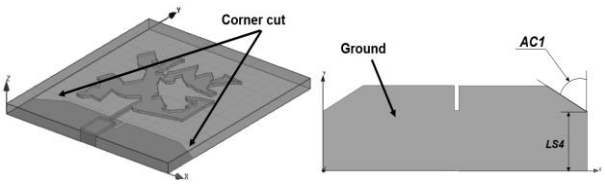

Fig. 12. Ground with corner cutouts.

The next obvious step towards optimizing the antenna geometry was scaling it up in the direction of increasing its size to cover cellular frequencies below 2.4 GHz.

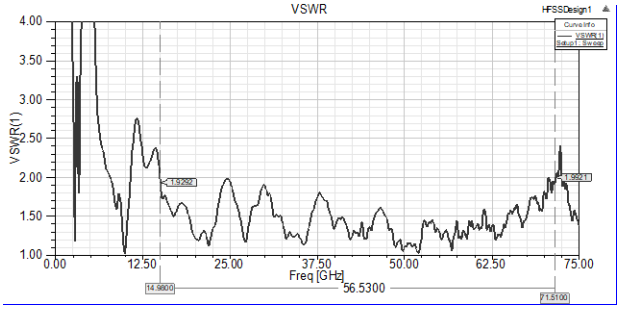

Fig. 13. Frequency dependence of VSWR of a chaotic antenna at *AC1* = 60 deg, *LS4* = 6.4 mm.

The scale factor values varied from x1.2 to x1.4. Such a range of this parameter was chosen to take into account the limitations on the external dimensions of the substrate (the antenna should not go beyond its limits). However, this procedure did not have a significant effect. It turned out that because of the fractional values of the Cartesian coordinates of the vertices of a chaotic contour, its scaling occurs with errors that increase as the size conversion factor increases. In this case, the original outline of the antenna is distorted, which affects the deterioration of the previously achieved characteristics. Therefore, the scaling procedure was supplemented by varying the relative permittivity ε_r of the substrate. In the course of the research, it was found that an increase in ε_r predictably leads to a shift in the passbands to the lower frequency range, but at the same time, the working sections are split into several fragments. This forced additional iterations of the selection of the antenna and the feeder line matching parameters. On the other hand, the results obtained confirmed the possibility of adapting the geometry of a chaotic antenna to the required frequency ranges in the interests of certain communication standards.

As an example of the implementation of the parametric model of the proposed antenna with acceptable values of frequency characteristics, a variant of the geometry of the feeder line matching transformer, which is presented in Table 1, can be indicated. In this case, the relative band δF in the range from 2.63 to 3.67 GHz is 33% (Fig. 14), and in the frequency segment from 9.66 to 153.13 GHz, respectively, δF = 143.466 / 81.3935 = 1.7626 (Fig. 15). It should be noted that with a little additional matching, this antenna covers the entire range of Wi-Fi 802.11y frequencies in the 3.6 GHz region and 4G cellular frequencies in the 2600 MHz range. This is achieved with a slight decrease in δF in the millimeter wavelength range.

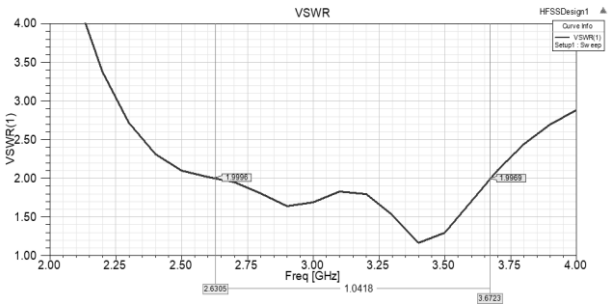

Fig. 14. The working frequency band of the chaotic antenna (Fig. 12) is in the 2.63 - 3.67 GHz range.

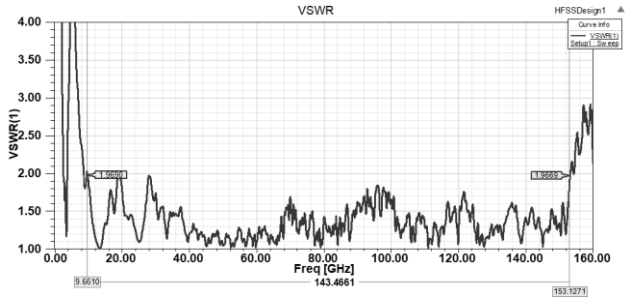

Fig. 15. Frequency dependence of VSWR of a chaotic antenna (Fig. 12).

TABLE II. ANTENNA PROPERTIES (FIG. 12) WHEN OPTIMIZING THE GEOMETRY OF THE FEEDER LINE

Element	Description
Substrate	FR4 (ε_r = 4.4), *T1* = 1.6 mm, *S1* = 36 mm, *S2* = 32 mm
Antenna	Cooper, *T2* = 0.385 mm
Feed line	Cooper, *LS1* = 6.9 mm, *WS1* = 3.65 mm, *LS2* = 4.15 mm, *WS2* = 1.1 mm
Ground	Cooper, *G1* = *S1*, *G2* = 9.2 mm, *LS3* = 2.7 mm, *WS3* = 1.14 mm, *LS4* = 6.4 mm, *AC1* = 60 deg

As you know, when designing printed antennas, it is necessary to take into account not only the skin effect, but also the features of the formation of the near electromagnetic field. This is especially important under the influence of edge effects with a screen shortened relative to the substrate (see Fig. 12). Therefore, an important stage of research was the assessment of the effect of the screen thickness, the feeder line, and the antenna itself. In the contrast to the antenna designs discussed above with a printed circuit thickness of 0.385 mm, for an example, simulation was carried out with an increase in the values of this parameter to 1.2 mm. Subsequent analysis made it possible to identify options for the geometry of the chaotic antenna, which have bandwidths in the standardized ranges of mobile communication systems from 4G (2600 MHz) to likely frequencies for 6G. One of the variants of such an antenna is shown in Fig. 16 and tab. 3 with characteristics in fig. 17, 18.

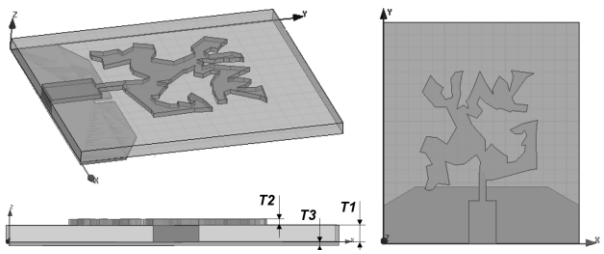

Fig. 16. The geometry of the chaotic antenna according to table. 3.

TABLE III. ANTENNA PROPERTIES (FIG. 16) WHEN OPTIMIZING THE GEOMETRY OF THE FEEDER LINE

Element	Description
Substrate	FR4 (ε_r = 4.4), *T1* = 1.6 mm, *S1* = 36 mm, *S2* = 32 mm
Antenna	Cooper, *T2* = 0.65 mm
Feed line	Cooper, *LS1* = 6.9 mm, *WS1* = 3.65 mm, *LS2* = 4.15 mm, *WS2* = 1.1 mm
Ground	Cooper, *G1* = *S1*, *G2* = 9.2 mm, *LS3* = 2.7 mm, *WS3* = 1.14 mm, *LS4* = 6.4 mm, *AC1* = 60 deg

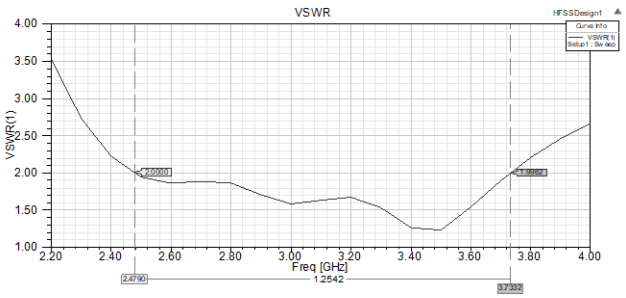

Fig. 17. Frequency dependence of VSWR of a chaotic antenna (Table 3).

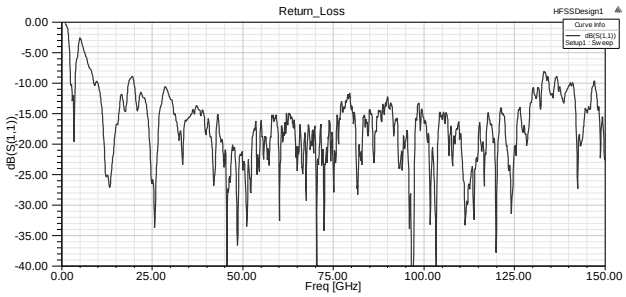

Fig. 18. Frequency dependence of the RL of a chaotic antenna (Table 3).

As you know, the widespread development of the Internet of Things is associated not only with NB-IoT, but also with other network technologies. Therefore, at the final stage of research, several versions of a chaotic antenna were obtained, which covers the 2.4 GHz range. The design parameters of one of such antennas and its characteristics are presented in the table. 4 and fig. 19 - 21.

TABLE IV. ANTENNA OPTION THAT SUPPORTS 2.4 GHZ

Element	Description
Substrate	FR4 (ε_r = 4.4), *T1* = 1.6 mm, *S1* = 36 mm, *S2* = 32 mm
Antenna	Cooper, *T2* = 0.6 mm
Feed line	Cooper, *LS1* = 6.9 mm, *WS1* = 4.45 mm, *LS2* = 4.15 mm, *WS2* = 1.1 mm
Ground	Cooper, *G1* = *S1*, *G2* = 9.2 mm, *T3* = 0.35 mm, *LS3* = 2.6 mm, *WS3* = 1.14 mm, *LS4* = 6.2 mm, *AC1* = 60 deg

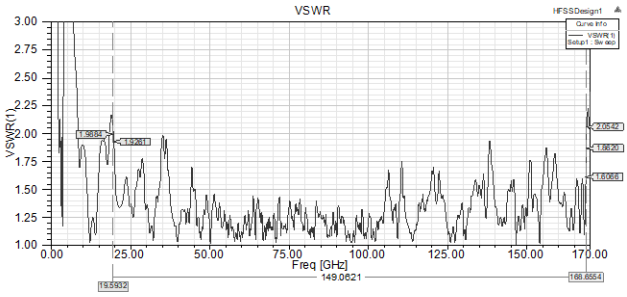

Fig. 19. Frequency dependence of VSWR of a chaotic antenna (Table 4).

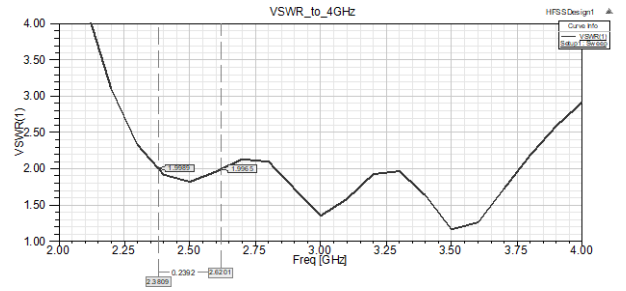

Fig. 20. Detailing of the Fig. 19.

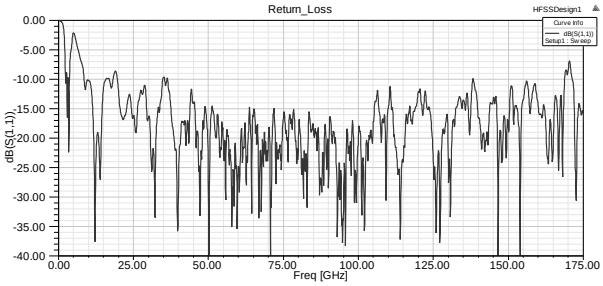

Fig. 21. Frequency dependence of the RL of a chaotic antenna (Table 4).

V. Perspectives of Further Reseach

Further research should be focused on the finding of optimal parameters for feeder lines, substrate, and screen, as well as on modeling other variants of chaotic antennas synthesized using the ant's optimization algorithm.

In turn, taking into account the use of mobile communication systems of MIMO and Massive MIMO technologies, it is advisable to form recommendations for the corresponding antennas arrays.

VI. Conclusions

The obtained designs of printed antennas make it possible to combine 5G [16] and 6G communication systems with 4G facilities in the 2600 MHz range [17], as well as with Wi-Fi systems (2400 - 2483.5 MHz) [18], Bluetooth (2402 - 2480 MHz) [19], Zegbee (2405 - 2485 MHz) [19]. In the addition, antenna solutions, whose characteristics are shown in Fig. 17, 20 are applicable for operation in the 3.6 GHz band (3657.5 - 3690 MHz), used in the USA for Wi-Fi systems of the 802.11y standard [20]. By their frequency properties, these antennas represent an alternative to printed emitters synthesized on the basis of genetic optimization algorithms [21].

Since the proposed variants of chaotic antennas will have in the millimeter wavelength range a rather narrow beam pattern compared to the lower frequency range, such antennas can be used for radio relay data transmission channels that collect an information from remote IoT systems in the 2.4 and 3.6 GHz bands. If it is necessary to cover the lower segments of the frequency spectrum, the presented designs can be scaled with an increase in their geometric dimensions and subsequent coordination.

References

[1] Z.E. Ankarali, B. Peköz and H. Arslan, “Flexible Radio Access Beyond 5G: A Future Projection on Waveform, Numerology, and Frame Design Principles”, *IEEE Access*, vol. 5, 2017.

[2] T.S. Rappaport, Y. Xing, O. Kanhere et al., “Wireless communications and applications above 100 GHz: Opportunities and challenges for 6G and beyond”, *IEEE Access*, vol. 7, pp. 78729-78757, 2019.

[3] M.H. Alsharif, M.A. Albreem, A.A. Solyman and Sunghwan Kim. “Toward 6G Communication Networks: Terahertz Frequency Challenges and Open Research Issues”, *Computers, Materials & Continua*, vol. 66, no.3, pp. 2821-2842, 2021. DOI: https://doi.org/10.32604/cmc.2021.013176.

[4] S. Tripathi, N.V. Sabu, A.K. Gupta et al., Millimeter-wave and Terahertz Spectrum for 6G Wireless, in Book *“6G Mobile Wireless Networks”*. Springer, 2021. Available: https://arxiv.org/abs/2102.10267.

[5] V.I. Slyusar, “Dijelektricheskie rezonatornye antenny. Malye razmery, bol'shie vozmozhnosti” [Dielectric resonator antennas. Small size, big possibilities], *Electronics: science, technology, business*, no.2, pp. 28-37, 2007. (In Russian).

[6] C.A. Balanis, Antenna Theory: Analysis and Design. 3rd ed. Hoboken, NJ: John Wiley, 2005.

[7] N.K. Darimireddy, R.R. Reddy, and A.M. Prasad, “A Miniaturized Hexagonal-Triangular Fractal Antenna for Wide-Band Applications”, *IEEE Antennas and Propagation Magazine*, pp. 104-110, April 2018. DOI: https://doi.org/10.1109/MAP.2018.2796441.

[8] S.Y. Ermolaev and V.I. Slyusar, “Antenna synthesis based on the ant colony optimization algorithm” in *IEEE 7th Int. Conf. on Antenna Theory and Techniques*, Lviv, Ukraine, October 2009, pp. 298-300.

[9] S.Y. Ermolaev and V.I. Slyusar, “Sintez antenn na osnove murav'inyh algoritmov optimizacii” [Antenna synthesis based on ant optimization algorithms] in *19th Int. Conf. SVCh-tehnika i telekommunikacionnye tehnologii* [*Microwave and telecommunication technologies*], Sevastopol, Ukraine, Septober 2009, pp. 431-432. (In Russian).

[10] A.I. Minochkin, V.I. Rudakov and V.I. Slyusar, *Osnovy voyenno-tekhnicheskikh issledovanii. Teoriia i prilozheniia: T. 2. Sintez sredstv informatsionnogo obespecheniia vooruzheniia i voennoi tekhniki* [*Theoretical bases of military-technical researches*]. Vol. 2. Kyiv, Ukraine, 2012, pp. 7-98, 354-521. (In Russian).

[11] A.I. Abdullahi, O.A. Rabiat and S.O. Sowole, “Vehicle Routing Problem with Exact Methods”, *IOSR Journal of Mathematics*, vol. 15, Issue 3, pp. 5-15, June 2019. DOI: https://doi.org/10.9790/5728-1503030515.

[12] S.E. Bankov and A.A. Kurushin, *Raschet antenn i SVCH struktur s pomoshchyu HFSS Ansoft* [*Calculation of antennas and microwave structures using HFSS Ansoft*], Moscow, Russia: ZAO NPP “Rodnik”, 2009, pp. 207, 208. (In Russian).

[13] I. Sliusar, V. Slyusar, S. Voloshko, A. Zinchenko and Y. Utkin, “Synthesis of a Broadband Ring Antenna of a Two-Tape Design” in *IEEE 12th Int. Conf. on Antenna Theory and Techniques*, Kharkiv, Ukraine, June 2020, pp. 161-165. DOI: https://doi.org/10.1109/UkrMW49653.2020.9252793.

[14] I. Sliusar, V. Slyusar, S. Voloshko and V. Smolyar, “Synthesis of quasi-fractal hemispherical dielectric resonator antennas”, in *IEEE 5th International ScientificPractical Conference Problems of Infocommunications. Science and Technology*, Kharkov, Ukraine, October 2018, pp. 313-316.

[15] Assessment of Ultra-Wideband (UWB) Technology. OSD/DARPA Ultra-Wideband Radar Review Panel, Battelle Tactical Technology Center, Contract No. DAAH01-88-C-0131, ARPA Order 6049. July 13, 1990.

[16] 5G NR (Rel-15). Available: https://www.3gpp.org/lte-2.

[17] 4th Generation (LTE). Available: https://www.etsi.org/technologies/mobile/4G.

[18] IEEE 802.11-2020. Available: https://standards.ieee.org/standard/802_11-2020.html

[19] V.M. Vishnevsky, A.I. Liachov, S.L. Portnoj et al., *Shirokopolosnye besprovodnye seti peredachi informacii* [*Broadband wireless communication networks*], Moscow, Russia: Technosphera, 2005, pp. 524-526. (In Russian).

[20] IEEE 802.11y-2008. Available: https://standards.ieee.org/standard/802_11y-2008.html.

[21] V.I. Slyusar, “Antenna Synthesis Based on the Genetic Algorithm”, Last mile (The Addition of Journal "Electronics: Science, Technology, Business"), no.1, pp. 22-25, 2009. (In Russian).